TOWARDS A NOVEL PERCEPTUAL COLOR DIFFERENCE METRIC USING CIRCULAR PROCESSING OF HUE COMPONENTS

Dohyoung Lee, Konstantinos N. Plataniotis

Multimedia Lab, The Edward S. Rogers Department of Electrical and Computer Engineering,
University of Toronto, 10 King's College Road, Toronto, Canada

ABSTRACT

This paper introduces a novel metric for image difference prediction, capable of handling color data. The proposed metric, namely, color difference index based on circular hue, is a full-reference based scheme, which independently processes achromatic and chromatic differences of two input color images. Within the framework, chromatic information is analyzed using two perceptual attributes, hue and chroma information, simulating human visual system mechanism. Unlike conventional approaches where the periodic nature of hue is disregarded, we propose to estimate hue difference by adopting theory of circular statistics. Performance of the proposed solution is validated using benchmark image quality assessment databases. Experimental results indicate the effectiveness of the proposed metric against a wide range of distortions, especially on chromatic distortions, making it better suited for color gamut mapping applications.

***Index Terms*—** color image, perceptual image difference, hue, angular data, circular statistics, color gamut mapping

1. INTRODUCTION

Throughout the last few decades, we have witnessed rapid proliferation of color imaging devices and color contents in a wide variety of multimedia communication systems, replacing their conventional grayscale counterparts. With such transition, demand for a computational metric, capable of estimating perceived color difference in visual data has increased, since it can replace cumbersome and time-consuming subjective assessment in real-time automated systems. For example, image difference metric can be exploited in color gamut mapping modules [1] for consistent color reproduction over different platforms. Since the main purpose of gamut mapping is to adjust color data according to the gamut of the target system without introducing noticeable difference, such objective measure can be effectively used in optimization of gamut mapping parameters [2].

Numerous techniques have been proposed to predict perceived difference in visual data [3, 4, 5]. Although the simplest computational tool to analyze image difference is the Mean Squared Error (MSE), it has been criticized for its pool performance from a perceptual point of view. Instead, a full-reference (FR) metric which attempts to incorporate structural information in image comparison, the Structural Similarity (SSIM) index [6] has received considerable attention from research community due to its high correlation with perceived image similarity and simple mathematical formulation. Under an assumption that human visual system (HVS) is highly sensitive to structural distortion, SSIM estimates perceived difference between two images by examining three complementary components, luminance, contrast, and structure in grayscale domain. Several extensions have been introduced from the baseline SSIM, such as the multiscale SSIM (MSSIM) [7], the image gradient SSIM [8], as well as the texture feature SSIM [9]. However, aforementioned variants are less suitable to handle color images exhibiting chromatic deviation, since they disregard contribution of chromatic information in perceived image difference. The most fundamental tools to measure difference of two visual stimuli are CIE color difference equations, e.g. CIEDE2000 [10]. Although they are useful for predicting perceived difference of two simple color patches, there is no guarantee that they work well with complex real-world image data. In principle, SSIM can be simply applied to individual RGB channels and each channel score can be combined to quantify overall difference between two color images. Since such direct extension is suboptimal in predicting perceived difference, more sophisticated approaches exploiting various properties of color perception have been proposed [11, 12, 13]. For instance, Toet and Lucassen [11] applied SSIM to a perceptually decorrelated $l\alpha\beta$ space to simulate the retinal image processing of HVS. Recently, Lissner et al. [13] proposed the image difference measure (IDM), which compares two images in perceptually uniform space, namely LAB2000HL [14] using three perceptual attributes, hue, chroma, and lightness components under SSIM framework.

In this paper, we introduce a novel image difference metric, namely color difference index based on circular hue ($\mathrm{CDI_{CH}}$),which independently processes achromatic and chromatic components of image data, adopting the retinal process of HVS. Chromatic component is further characterized by two perceptual attributes, hue and chroma, where hue corresponds to an angular measure around the achromatic axis, and chroma corresponds to the distance from the achromatic axis. Especially, hue direction comparison term based on the theory of circular statistics [15, 16], a measure that quantifies the difference between local hue information between two color data, is introduced as the primary feature in the proposed scheme. This term takes into account the periodic nature of angular hue, which is often neglected in general image processing applications.

The rest of this paper is organized as follows. Section 2 presents background information related to circular statistics. Section 3 presents the proposed metric in detail. Experimental results are reported in Section 4 and conclusion is drawn in Section 5.

2. CIRCULAR DATA AND MEAN DIRECTION

Although we generally deal with data whose domain lie in a straight line during most of image analysis, there exists certain applications that require us to process angular data, such as hue in cylindrical color systems. In this section, we provide some basic definitions of circular statistics used in our proposed metric, that allow us to process such angular data.

978-1-4799-2893-4/14/$31.00 ©2014 IEEE

Let's assume that we have N angular observations $\theta_1, \ldots, \theta_N$, where $\theta_i \in [0, 360°)$. Initially, sample data are transformed to unit vectors in two-dimensional plane, represented by sample points $P_i = [\cos\theta_i, \sin\theta_i]^T$ on a unit circle as shown in Fig 1.

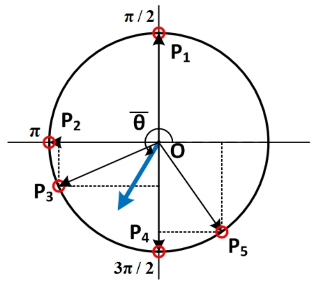

Fig. 1. Sample mean direction $\overline{\theta}$ of five angular data, $P_1, \ldots, P_5$, represented on a unit circle

Then we obtain the resultant vector of N unit vectors from the origin by summing them component wise:

$$R = \Big(\sum_{i=1} \cos\theta_i, \sum_{i=1} \sin\theta_i\Big) = \Big(C_N, S_N\Big) \quad (1)$$

The *sample mean direction* $\overline{\theta}$, the average angle of angular samples, can be computed from the direction of resultant vector $\vec{R}$ as follows:

$$\overline{\theta} = \arctan(C_N/S_N) \quad (2)$$

3. PROPOSED COLOR DIFFERENCE METRIC

It is well known that human eye processes the retinal image in three color channels, one achromatic and two chromatic channels (opponent color) [17]. Under an assumption that achromatic and chromatic components contribute independently to overall perceived color appearance, our framework translate input color signal to the domain where both components are easily accessible. Then, achromatic and chromatic components are compared independently to generate difference maps (i.e. matrices composed of local difference scores) of individual channels. Afterwards, the map is translated into a single score by applying spatial pooling to each comparison map, followed by component pooling. It should be noted that the proposed scheme relies on simple low-level visual features of color images rather than complex semantics, and thus, it is computationally efficient and widely applicable for general color images.

The inputs to the system are two RGB color images, $\mathbf{X}$ and $\mathbf{Y}$ ($\mathbf{X}, \mathbf{Y} : \mathbb{R}^2 \rightarrow \mathbb{R}^3$), which are assumed to be consistent in spatial resolution and bit depth, as well as properly aligned. The output of the system $CDI_{CH}(\mathbf{X}, \mathbf{Y})$ is a measure of color difference between two images ($CDI_{CH}(\mathbf{X}, \mathbf{Y}) \geq 0$,where 0 indicates that both are identical images). The block diagram is illustrated in Fig 2.

3.1. Color Space Conversion

Despite its dominant usage in image representation, RGB domain is not suitable to perform perceptual color analysis due to its lack of correlation with visual perception. Hence, RGB image should be transformed to color space where convenient extraction of perceptual color attributes, e.g. hue, chroma, and lightness [18], is allowed. Aforementioned attributes are easily accessible from perceptual color systems, such as HSV [19], HSL, CIELAB, and S-CIELAB,

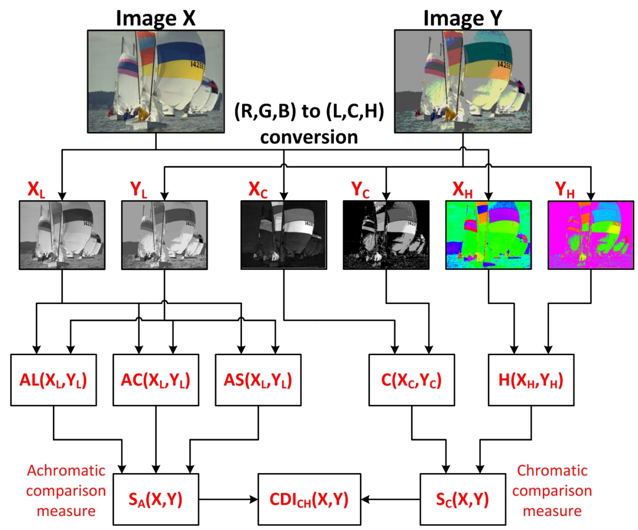

Fig. 2. Illustration of the CDI_{CH} index computation for given color images $\mathbf{X}$ and $\mathbf{Y}$ (Terminologies are explained in section 3.2)

rather than rectangular system. Among perceptual attributes, two chromatic ones, hue and chroma characterize the color vector by means of vector direction angle and vector magnitude in a polar coordinate. The main properties of each component are as follows:

- Hue : an attribute related to dominant wavelength of color signal, and represented by angle, i.e. $H \in [0, 360°)$, in the chromatic plane around the achromatic axis (i.e. lightness $L*$ axis). Circular processing is required to handle hue data due to periodicity.
- Chroma : an attribute related to relative colorfulness of the color, which is represented by its magnitude of projected color vector onto chromatic plane.

These two components play an important role to quantify the chromatic deviation in two image data, which occurs very often in color gamut mapping algorithms (GMA). For example, Zolliker's GMA [20] attempts to generate a gamut mapped image while preserving original local contrast, lightness, and saturation of the original image, which often lead to shifts in hue components.

In the proposed scheme, we make use of S-CIELAB [21], a spatial extension of CIELAB, for following reasons: i) it is a uniform color coordinate designed for color difference analysis, where its values describe the perceived differences between stimuli, ii) S-CIELAB exploits a spatial pre-processor to approximate the contrast sensitivity function (CSF) of HVS, allowing for normalization of visual information based on viewing distance. In S-CIELAB, color signal is represented with three terms, lightness L^*, redness-greenness a^*, and blueness-yellowness b^*. Hue H and chroma C, can be derived from two chromaticity terms a^* and b^* as follows:

$$H = \arctan(b^*/a^*), \;\; C = \sqrt{a^{*2} + b^{*2}} \quad (3)$$

3.2. Component Specific Difference Map Estimation

The proposed framework compares chromatic and achromatic components of given input images independently. Since different image regions may undergo different types of distortion, we initially measure perceived difference within local regions. In this section, we develop several comparison terms to measure perceived difference between two corresponding local patches of input images, $\mathbf{x}$ and $\mathbf{y}$. Here, we assume that each local patch contains N pixels, i.e. $\mathbf{x} = \{x_i | i = 1, \ldots, N\}, \mathbf{y} = \{y_i | i = 1, \ldots, N\}$.

To quantify hue difference between $\mathbf{x}$ and $\mathbf{y}$, we introduce *hue direction* comparison term $H(\mathbf{x}, \mathbf{y}) : \mathbb{R}^N \times \mathbb{R}^N \to \mathbb{R}$, given by:

$$H(\mathbf{x}, \mathbf{y}) = \frac{2\overline{\theta}_{\mathbf{x},H} \cdot \overline{\theta}_{\mathbf{y},H} + K_H}{\overline{\theta}^2_{\mathbf{x},H} + \overline{\theta}^2_{\mathbf{y},H} + K_H} \tag{4}$$

where $\overline{\theta}_{\mathbf{x},H}$ and $\overline{\theta}_{\mathbf{y},H}$ are the circular mean of hue values (refer to (2)) for the central pixel of image patches $\mathbf{x}$ and $\mathbf{y}$, and K_H is a small positive constant which prevents the denominator being zero (Note that suggested values for K_H vary depending on the dynamic range of hue values. We use $K_H = (360 \cdot 0.01)^2$ for hue represented in degree). This term essentially evaluates how close the average hue value both local patches have, which is an important perceptual cue for chromatic distortion. As explained previously, it is important to use circular mean instead of conventional arithmetic mean for appropriate treatment of angular data. $H(\mathbf{x}, \mathbf{y})$ is quantified between $[0, 1]$ where 1 indicates equivalence.

Similarly, chroma comparison term $C(\mathbf{x}, \mathbf{y}) : \mathbb{R}^N \times \mathbb{R}^N \to \mathbb{R}$ is defined as:

$$C(\mathbf{x}, \mathbf{y}) = \frac{2\mu_{\mathbf{x},C} \cdot \mu_{\mathbf{y},C} + K_C}{\mu^2_{\mathbf{x},C} + \mu^2_{\mathbf{y},C} + K_C} \tag{5}$$

where $\mu_{\mathbf{x},C}$ and $\mu_{\mathbf{y},C}$ are the arithmatic mean chroma values for the central pixel of image patches $\mathbf{x}$ and $\mathbf{y}$, respectively, and K_C is a positive constant for numerical stability.

For comparison of achromatic component, we directly adopt the original SSIM metric [6] on lightness channels due to its reasonable performance in predicting perceived difference and computational efficiency. In other words, three achromatic comparison maps are generated; each represents mean luminance distortion, contrast distortion, and loss of linear correlation as follows:

$$\begin{aligned} AL(\mathbf{x}, \mathbf{y}) &= \frac{2\mu_{\mathbf{x},L}\mu_{\mathbf{y},L} + K_{L1}}{\mu^2_{\mathbf{x},L} + \mu^2_{\mathbf{y},L} + K_{L1}} \\ AC(\mathbf{x}, \mathbf{y}) &= \frac{2\sigma_{\mathbf{x},L}\sigma_{\mathbf{y},L} + K_{L2}}{\sigma^2_{\mathbf{x},L} + \sigma^2_{\mathbf{y},L} + K_{L2}} \\ AS(\mathbf{x}, \mathbf{y}) &= \frac{\sigma_{\mathbf{xy},L} + K_{L3}}{\sigma_{\mathbf{x},L}\sigma_{\mathbf{y},L} + K_{L3}} \end{aligned} \tag{6}$$

where $\sigma_{\mathbf{x},L}$, $\sigma_{\mathbf{y},L}$ and $\sigma_{\mathbf{xy},L}$ denote the local standard deviations and cross correlation between lightness channels of two corresponding patches; K_{L1}, K_{L2}, and K_{L3} are small constants. Here, we set them as $K_{L1} = (100 \cdot 0.01)^2$, $K_{L2} = (100 \cdot 0.03)^2$, and $K_{L3} = K_{L2}/2$, adopting the recommendation from [7].

3.3. Difference Score Pooling

In order to derive a single numerical score that represents overall perceived difference, we need to combine individual local measurement from previously obtained five maps. In the proposed framework, we initially perform a spatial pooling of each comparison maps, followed by a component pooling of each channel score into final value. This pooling sequence is inherited from [13], since it yields better prediction performance than the pooling sequence in reverse order, i.e. component pooling followed by spatial pooling.

For instance, hue direction map is converted into hue direction similarity score, $H(\mathbf{X}, \mathbf{Y}) : \mathbb{R}^{h \times w} \times \mathbb{R}^{h \times w} \to \mathbb{R}$ (h and w indicates the height and width of input images) given by:

$$H(\mathbf{X}, \mathbf{Y}) = \frac{1}{h \times w} \sum_{i=1}^{h} \sum_{j=1}^{w} H(\mathbf{x}_{i,j}, \mathbf{y}_{i,j}) \tag{7}$$

where $\mathbf{x}_{i,j}$ and $\mathbf{y}_{i,j}$ denote local image patches of two image $\mathbf{X}$, $\mathbf{Y}$, centered at pixel location (i, j). Although we assumed that every region is equally significant here, a spatially varying weighting scheme [22, 23] based on visual saliency is also applicable. In similar manner, scores for other comparison maps can be computed.

From the component specific scores, we can evaluate two scores representing the degree of similarity in chromatic and achromatic components, namely *chromatic similarity* and *achromatic similarity* scores given by:

$$\begin{aligned} S_C(\mathbf{X}, \mathbf{Y}) &= H(\mathbf{X}, \mathbf{Y}) \cdot C(\mathbf{X}, \mathbf{Y}) \\ S_A(\mathbf{X}, \mathbf{Y}) &= AL(\mathbf{X}, \mathbf{Y}) \cdot AC(\mathbf{X}, \mathbf{Y}) \cdot AS(\mathbf{X}, \mathbf{Y}) \end{aligned} \tag{8}$$

Finally, the CDI_{CH} can be obtained by incorporating the chromatic and achromatic similarity scores as follows:

$$CDI_{CH}(\mathbf{X}, \mathbf{Y}) = 1 - [S_A(\mathbf{X}, \mathbf{Y})]^{\alpha_A} \cdot [S_C(\mathbf{X}, \mathbf{Y})]^{\alpha_C} \tag{9}$$

where nonnegative parameters α_A and α_C adjusts the significance of achromatic and chromatic components in overall difference. We set $\alpha_A = \alpha_C = 1$ in this paper for simplicity. It should be noted that both parameters can be adjusted depending on target application. We may set $\alpha_A > \alpha_C$ as HVS is generally more sensitive to achromatic distortion (e.g. chrominance component subsampling in image compression standard), but in color gamut mapping scenario, increased significance of chromatic term would be more beneficial).

4. EXPERIMENTAL RESULTS

In order to evaluate whether the proposed metric is statistically consistent with human visual perception, Tampere Image Database (TID2013) [24] is used, which consists of 3000 distorted images obtained from 25 original images (containing 24 natural images from the Kodak database, and one artificially generated image) with 24 types of distortions over 5 distortion levels. Each image in TID2013 DB is acquired in 8-bit RGB with 512x384 resolution, formatted in BMP. This database is chosen since: i) it is widely used DB for perceptual image comparison research covering a wide range of distortions from chromatic to more generic ones, ii) it is annotated with mean opinion score (MOS), facilitating convenient benchmark of the proposed scheme with other algorithms.

To facilitate systematic evaluation of the framework, following experiments are conducted: i) evaluation of the proposed metric on sample images exhibiting chromatic distortions, ii) evaluation on sample images exhibiting generic distortions. Hence, TID2013 DB is divided into two subsets, the *color subset* exhibiting chromatic distortion (750 images containing JPEG compression distortion, color saturation adjustment, color quantization with dither, chromatic aberrations, and so forth; distortion type 2,7,10,18,22,23 in TID2013) and the *non-color subset* containing the rest of distorted images in TID2013. Validation is performed by comparing difference prediction results with provided subjective groundtruth. Two commonly used evaluation criteria are employed including Spearman's rank-order correlation coefficient (SCC) and Kendall's rank-order correlation coefficient (KCC). Both measures only take into consideration the rank of the score and neglect the relative distance between scores. Note that a better metric has a higher SCC and KCC values (1 indicates the perfect prediction).

Block size	TID2013 Color Set						TID2013 Non-color Set					
	CIELAB		S-CIELAB		HSV		CIELAB		S-CIELAB		HSV	
	SCC	KCC	SCC	KCC	SCC	KCC	SCC	KCC	SCC	KCC	SCC	KCC
3x3	0.735	0.534	0.875	0.676	0.669	0.471	0.505	0.352	0.739	0.555	0.422	0.289
7x7	0.761	0.557	0.864	0.660	0.735	0.527	0.568	0.404	0.735	0.546	0.494	0.342
11x11	0.777	0.571	0.870	0.668	0.747	0.538	0.599	0.429	0.745	0.558	0.509	0.353

Table 1. Performance of the CDI_{CH} metric on color and non-color subsets of TID2013 DB using various color systems and local patch sizes

Table 1 compares SCC and KCC performances of our proposed metric using three commonly used color representations (all of them allows for access to hue), along with varying local patch sizes. Since exact viewing condition for TID2013 DB is not provided, we simply assumed a visual angle of 25 cycles per degree for configuration of S-CIELAB (roughly simulating viewing distance of 20 inches from a monitor, which is capable of displaying 72 pixels-per-inch). Superior performance of S-CIELAB against CIELAB implies that the viewing distance normalization does enhance prediction performance of the metric. In addition, normalization effectively minimizes the dependence of local patch size on the performance as S-CIELAB yields relatively consistent performance across different patch sizes. HSV system, a close approximation of CIELAB, yields suboptimal performance and thus, it is not recommended for perceptual difference analysis unless low-complexity alternative is required. Hence, it justifies the use of S-CIELAB in our proposed metric.

Benchmark Metric	TID2013 Color set		TID2013 Non-color set	
	SCC	KCC	SCC	KCC
SSIM [6]	0.506	0.382	0.669	0.486
MSSIM [7]	0.566	0.456	0.853	0.659
$PSNR_c$	0.734	0.536	0.671	0.482
$FSIM_c$ [12]	0.775	0.593	0.874	0.691
IDM [13]	0.852	0.650	0.766	0.568
CDI_{CH}	0.870	0.668	0.745	0.558

Table 2. Performance comparison for image difference measures on two subsets of TID2013 DB (11x11 window is selected for CDI_{CH} due to its overall reliable performance across both subsets)

In order to provide overall comparative performance of the proposed scheme against other existing metrics, Table 2 demonstrates KCC and SCC results over two subsets of TID2013. All benchmark metrics except basic SSIM [6] and MSSIM [7], make use of color information in different color space and processing sequence. $FSIM_c$ [12] estimates chromatic difference using I,Q components of YIQ color space and further employs low-level features, namely, phase congruency (PC) and gradient magnitude (GM), to predict overall perceived difference. It is included in comparison due to its state-of-the-art performance in perceptual image analysis [4, 24]. Result in Table 2 shows that the proposed metric outperforms all other methods on color set of TID2013 DB, demonstrating its superior performance in estimating perceived difference caused by deviation in chromaticity. The proposed metric performs less effective than some metrics on non-color set of TID2013. It is attributed for additional complex operations that other metrics rely on, e.g. the weighted spatial pooling strategy in $FSIM_c$, and the multiscale extraction of comparison maps in MSSIM. Therefore, there is still room for improvement by incorporating similar advanced strategies.

The proposed FR metric would be useful for automatic calibration of color gamut mapping systems for two reasons: i) full resolution of both color images to be compare are available from users, ii) chromatic difference between both signals is more significant than conventional achromatic difference (Fig 3 demonstrates an example of significant hue and chroma deviations occurred during gamut mapping process)

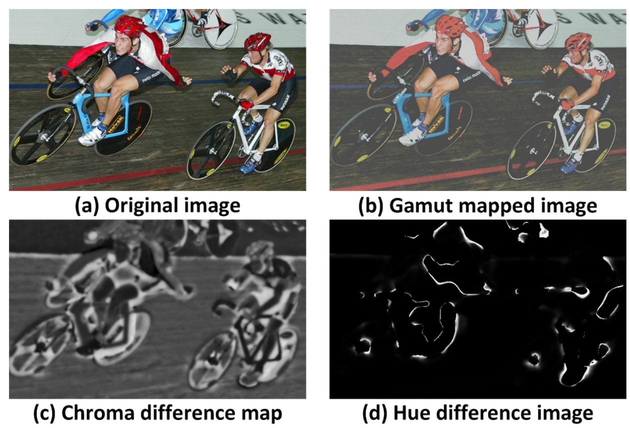

Fig. 3. Chromatic difference maps generated from the proposed metric by comparing the sample image from [25] and the adjusted image using Zolliker's GMA [20] (lighter pixels indicate highly different regions, while darker pixels indicate similar regions)

5. CONCLUSION

In this paper, we have introduced a novel computational metric to predict perceived image difference between two color images. To achieve good correlation between subjective assessment score and the proposed metric, we makes use of complementary information from three perceptual attributes, hue, chroma, and lightness. Especially, hue signal, representing the dominant wavelength of the color signal, is processed using circular statistics to ensure the periodicity of angular data is properly taken into consideration. Experimental result demonstrates that the proposed metric accurately predicts perceived difference in image data exhibiting chromatic distortion, making it suitable for color gamut mapping applications.

6. REFERENCES

[1] Ján Morovič, *Color Gamut Mapping*, John Wiley & Sons, Ltd, 2008.

[2] P. Zolliker, Z. Barańczuk, and J. Giesen, "Image Fusion for optimizing Gamut Mapping," in *Proceedings of the 19th Color Imaging Conference (CIC 2011)*, 2011, pp. 109–114.

[3] Weisi Lin and C.-C. Jay Kuo, "Perceptual Visual Quality Metrics: A Survey," *Journal of Visual Communication and Image Representation*, vol. 22, no. 4, pp. 297 – 312, 2011.

[4] Lin Zhang, Lei Zhang, Xuanqin Mou, and David Zhang, "A Comprehensive Evaluation of Full Reference Image Quality Assessment Algorithms," in *Proceedings of the IEEE International Conference on Image Processing (ICIP)*, 2012, pp. 1477–1480.

[5] Damon M Chandler, "Seven Challenges in Image Quality Assessment: Past, Present, and Future Research," *ISRN Signal Processing*, vol. 2013, 2013.

[6] Zhou Wang, Alan C Bovik, Hamid Rahim Sheikh, and Eero P Simoncelli, "Image Quality Assessment: From Error Visibility to Structural Similarity," *IEEE Transactions on Image Processing*, vol. 13, no. 4, pp. 600–612, Apr. 2004.

[7] Zhou Wang, Eero P Simoncelli, and Alan C Bovik, "Multiscale Structural Similarity for Image Quality Assessment," in *Proceedings of the IEEE Asilomar Conference on Signals, Systems, and Computers*, 2003, vol. 2, pp. 9–13.

[8] Anmin Liu, Weisi Lin, and Manish Narwaria, "Image Quality Assessment Based on Gradient Similarity," *IEEE Transactions on Image Processing*, vol. 21, no. 4, pp. 1500–1512, 2012.

[9] Jana Zujovic, Thrasyvoulos N Pappas, and David L Neuhoff, "Structural Texture Similarity Metrics for Image Analysis and Retrieval," *IEEE Transactions on Image Processing*, vol. 22, no. 7, pp. 2545–2558, July 2013.

[10] M. R. Luo, G. Cui, and B. Rigg, "The development of the CIE 2000 colour-difference formula: CIEDE2000," *Color Research & Application*, vol. 26, no. 5, pp. 340–350, 2001.

[11] Alexander Toet and Marcel P. Lucassen, "A New Universal Colour Image Fidelity Metric," *Displays*, vol. 24, no. 45, pp. 197 – 207, 2003.

[12] Lin Zhang, Lei Zhang, Xuanqin Mou, and David Zhang, "FSIM : A Feature Similarity Index for Image Quality Assessment," *IEEE Transactions on Image Processing*, vol. 20, no. 8, pp. 2378–2386, 2011.

[13] Ingmar Lissner, Jens Preiss, Philipp Urban, Matthias Scheller Lichtenauer, and Peter Zolliker, "Image Difference Prediction: From Grayscale to Color," *IEEE Transactions on Image Processing*, vol. 22, no. 2, pp. 435–446, Feb. 2013.

[14] Ingmar Lissner and Philipp Urban, "Toward a Unified Color Space for Perception Based Image Processing," *IEEE Transactions on Image Processing*, vol. 21, no. 3, pp. 1153–1168, 2012.

[15] Allan Hanbury, "Circular Statistics Applied to Colour Images," in *8th Computer Vision Winter Workshop*, 2003.

[16] Nikos Nikolaidis and Ioannis Pitas, "Nonlinear Processing and Analysis of Angular Signals," *IEEE Transactions on Signal Processing*, vol. 46, no. 12, pp. 3181–3194, 1998.

[17] Konstantinos N. Plataniotis and Anastasios N. Venetsanopoulos, *Color Image Processing and Applications*, Springer-Verlag New York, Inc., 2000.

[18] Mark D Fairchild, *Color Appearance Models*, John Wiley & Sons, Ltd, 2013.

[19] Alvy Ray Smith, "Color Gamut Transform Pairs," *ACM SIGGRAPH Computer Graphics*, 1978.

[20] P. Zolliker and K. Simon, "Retaining Local Image Information in Gamut Mapping Algorithms," *IEEE Transactions on Image Processing*, vol. 16, no. 3, pp. 664–672, 2007.

[21] X. Zhang and B. A. Wandell, "A Spatial Extension of CIELAB for Digital Color-Image Reproduction," *Journal of the Society for Information Display*, vol. 5, no. 1, pp. 61–63, 1997.

[22] Anan Guo, Debin Zhao, Shaohui Liu, and Guangyao Cao, "Fovea Based Image Quality Assessment," in *Proceedings of the SPIE*, July 2010, vol. 7744.

[23] Zhou Wang and Qiang Li, "Information Content Weighting for Perceptual Image Quality Assessment," *IEEE Transactions on Image Processing*, vol. 20, no. 5, pp. 1185–1198, May 2011.

[24] Nikolay Ponomarenko, Oleg Ieremeiev, Vladimir Lukin, Lina Jin, Karen Egiazarian, Jaakko Astola, Benoit Vozel, Kacem Chehdi, Marco Carli, Federica Battisti, and C.-C.Jay Kuo, "A New Color Image Database TID2013: Innovations and Results," in *Advanced Concepts for Intelligent Vision Systems*, vol. 8192 of *Lecture Notes in Computer Science*, pp. 402–413. Springer International Publishing, 2013.

[25] J. Giesen, E. Schuberth, K. Simon, P. Zolliker, and O. Zweifel, "Image-Dependent Gamut Mapping as Optimization Problem," *IEEE Transactions on Image Processing*, vol. 16, no. 10, pp. 2401–2410, 2007.